Displacement of weak rock joints under railway loading using numerical modelling

Rakesh Sai Malisetty & Buddhima Indraratna
Transport Research Centre, School of Civil and environmental engineering, University of Technology Sydney, Australia, rakeshsai.malisetty@uts.edu.au

Richard Kelly
SMEC Australia

ABSTRACT: The south-eastern coast of Australia is underlain by weak sandstone which can be found at shallow depths across Sydney metropolitan region. For railway infrastructure in this region, a significant challenge is posed by the presence of highly weathered joints that are prone to slip under railway loading. When oriented at a particular dip and strike combination, the impact of railway loading on the joint is maximum leading to joint displacements. This paper provides a review of the engineering characteristics of sandstone and the typical orientation of joints in the region. Then, railway track on jointed rock formation was modelled using finite element models by considering joint as a Coulomb frictional interface. For different loading conditions, joint displacements at different joint orientations were analysed to determine the critical joint orientation. When joints are shearing, differential settlements between sleepers and rails were observed in both lateral and longitudinal directions causing a twist in the sleeper-rail system. A detailed analysis of the influence of different ballast and rock subgrade conditions on joint displacements is presented in this paper highlighting their implications to track stability.

KEYWORDS: please provide a relevant keyword list (up to 5 keywords, single line only).

1 INTRODUCTION

Railways are an important mode of transport for the efficient supply of goods and bulk commodities across different parts of a country. In Australia, freight trains are often very heavy with the axle loads ranging from 25 T for coal wagons to 40 T for iron ore wagons. It is important that the differential settlements in a track should be kept minimum for optimal track performance (Selig and Waters, 1994). These differential settlements in a railway track are dependent on substructure characteristics such as the quality of ballast and subgrade layers.

Tracks on very soft subgrade soils such as marine clays have high potential of large displacements under railway loading which necessitates additional fill layers before ballast layers are laid upon (Indraratna et al., 2012). For locations where rock formations are found as subgrades, ballasted tracks are generally often constructed directly on the rock formations. However, if the rock formation is comprised of large discontinuities such as joints or fractures, the joint movements over a long period can affect the settlements in ballast layers leading to differential settlements in the tracks. Further, freight trains with heavy axle loads can also act as a potential cause for joint displacements. This can be possible if the underlying rock formation are highly weathered and fractured as found in Sydney basin.

Numerous laboratory and field investigations on Hawkesbury sandstone in Sydney region have found that class-IV sandstone formations at shallow depths are highly weathered and of low compressive strength going as low as 5-10 MPa (Pells, 2004, Bertuzzi, 2014, Keneti et al., 2021). Further, a number of sub-vertical joints were reportedly present at different orientations in the sandstone formations. Under conditions where these joints traverse the railway tracks, the joints displace causing excessive settlement of ballast than expected at certain locations. This behavior is further amplified when joints are old and smooth when the joint shear strength reduces and their susceptibility to slip increase.

Different numerical models can be employed to understand the behavior of rock masses under various loading environments. Because of a diverse variety of discontinuities in rock masses, it is important to carefully select the type of numerical analysis based on the scale of the model compared to the size of discontinuities (Bobet et al., 2009). Jing (2003) reported that Continuum models are deemed suitable when looking at intact rock systems or rock masses with persistent discontinuities which govern the behavior of the whole system. For rock masses with multiple discontinuities where rotation and separation of blocks are possible, distinct element methods are more appropriate. For the rock formation analysed in this study, joint is considered as a persistent joint which acts as a weakness plane along which the joint displacement can occur.

In this paper, the influence of static railway loads on a jointed rock formation is analysed where the ballasted track was constructed directly on rock formation. A full-scale model of a railway track is developed using three-dimensional Finite Element Mesh through commercially available software (ABAQUS). Different orientations of joints are analysed with different joint strength characteristics to evaluate the joint slip under static railway loads. The influence of joint slip on the differential settlements of railway track are analysed under different joint strength characteristics and orientations.

2 INFLUENCE OF JOINT ON THE SHEAR STRENGTH OF ROCK MASS

When a persistent weakness plane such as joint is present, the behavior of the rock mass is severely affected by the shear strength of the joint. This influence was investigated by several researchers where an intact rock with a single joint oriented at different joint dip angles was tested under triaxial compression conditions (Alejano et al., 2021, Tien and Kuo, 2001, Hoek and Brown, 1980). In all these tests, the joint was considered to be through-going oriented at an angle β with the major principal stress direction as shown in Fig. 1. Two types of failure modes were observed based on the orientation angle of the joint: sliding failure mode and non-sliding failure mode. In the first mode, the shear strength of the joint governs the overall strength behavior, while the second failure mode occurs at relatively high stresses where the failure happens in intact rock. Jaeger (1971) developed a theoretical model to predict the anisotropic strength of rock mass during the first failure mode using Eq.1 given as:

$$\sigma'_{1f} = \sigma'_3 + \frac{2(C+\sigma_3 \tan\emptyset)}{(1-\tan\emptyset \tan\beta)\sin 2\beta} \quad (1)$$

where, σ'_{1f} is the peak strength in major principal stress direction, σ'_3 is the minor principal stress or the confining stress of the sample, C and $\emptyset$ are the cohesion and friction coefficient on the joint, respectively. As seen in Fig. 1, the peak strength of the material at different confining stress reduces when the failure mode is through weak joint forming a U-shape curve with β. For cohesionless joints, a certain combination of $\emptyset$ and β will yield the range of discontinuity angles where failure occurs through sliding. At very steep and flat angles, the strength of intact rock governs the overall strength of the rock mass. Even though not quite distinguishable, the weakest joint plane occurs at $\beta = 45^0 + \emptyset/2$ and is independent of the applied confining stress on the rock specimen. However, the stress conditions under which Jaeger's theory is applicable is limited as the stress conditions in the field is rarely triaxial compression. A few studies (Tiwari and Rao, 2007, Faizi et al., 2020) have investigated the influence of intermediate principal stress on the anisotropic strength of the rock and reported that higher intermediate principal stresses tend to flatten the U-shape curve, suppressing the difference between different joint angles.

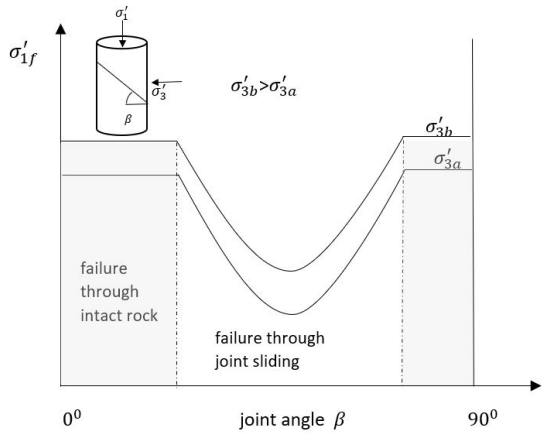

Figure 1. Representation of anisotropic strength of rock mass with a through-going joint

2.1. Strength of rock joints under shearing

In addition to the joint orientation, the strength of rock joints is also dependent on the frictional characteristics of the joint. It is well established that the extent and size of undulations on the joint surface affects the effective friction angle of the joint under shearing (Barton, 1973, Bandis et al., 1981, Indraratna et al., 1999). The influence of surface roughness is usually characterized using a Joint Roughness Coefficient (JRC) which can be determined by different geometrical estimation methods. The influence of JRC on the shear strength of the joint was proposed by Barton (1973) through various experimental tests and further modified by Barton and Bandis (1982) to include joint length and is given as:

$$\tau_{peak} = \sigma'_N \tan\left(\emptyset_0 + JRC_n \, x \, log\left(\frac{JCS}{\sigma'_N}\right)\right) \qquad (2)$$

where, τ_{peak} is the shear strength of the joint, σ'_N is the normal stress on the joint and JCS is the Joint Compressive Strength, usually taken as uniaxial compressive strength of the intact rock. JRC_n denotes the equivalent JRC of a rock joint with length L_n compared to the laboratory scale JRC_0 with a length of L_0 and is given as:

$$JRC_n = JRC_0 \left(\frac{L_n}{L_0}\right)^{-0.02JRC_0} \qquad (3)$$

3 NUMERICAL MODELLING OF RAILWAY TRACK ON JOINTED ROCK FORMATION

Figure 2 shows the FEM mesh of the railway track on jointed rock formation used in this study. Railway loading is simulated using a two-axle bogie with typical distance between axles of the bogie taken as 1.8m. The dimensions of individual track elements such as rails, sleepers and ballast are considered following Australian railway standards and are given in Table-1.

The total length of the track is taken as 10m encompassing 15 sleepers with a sleeper c/c spacing of 600mm and the width and depth of the track are taken as 6m. Geological investigations on class-IV Hawkesbury sandstone showed that the rock formation is divided into two cross-bedded layers with the bed thickness ranging from 2-6m. To consider this geological feature, the rock formation is modelled as 2 layers separated by a bedding plane with the thickness of top layer taken as 4m. A persistent rock joint is considered in the first rock layer with a dip and strike calculated as angles made by the joint with the horizontal and lateral planes as shown in Figure. In this study, the strike orientation of the joint is considered as 90 degrees, i.e., the joint is cutting through the joint laterally. The location of the joint is fixed to maintain the symmetricity of the sliding and resisting rock masses on either side of the joint. The track layers are modelled using 8-node brick elements (C3D8) and infinite elements are considered at the longitudinal edges and bottom surface to prevent wave reflection off the boundaries.

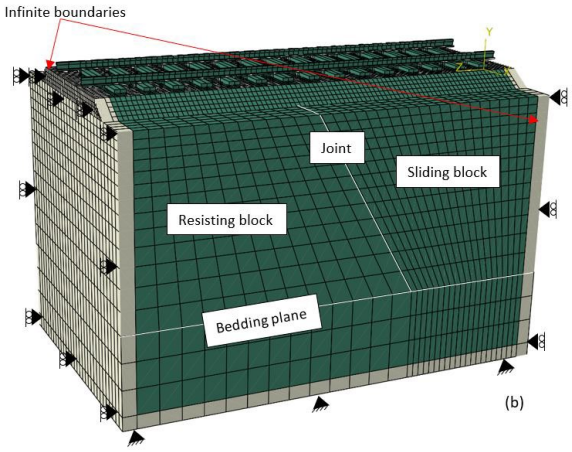

Figure 2. Three-dimensional mesh of the railway track on jointed rock formation analysed in this model.

A few approaches for modelling rock joints in finite element method using joint elements are available in literature. However, for simplicity the Coulomb friction model available in Abaqus is modified using Barton and Bandis (1982) non-linear strength criterion given in Eq. 2 to include the influence of JRC on the joint displacements. Elastic-perfectly plastic joint behavior is considered in this study, where the stiffness of the elastic response is dependent on Barton's peak shear strength (Eq.2) and critical strain of the joint (ϵ_{crit}) given in Table-1. Further, since JRC is direction dependent, the joint was considered isotropic with same frictional coefficients in both shearing directions on the joint plane.

Elastic parameters are assumed for rails and sleepers and elasto-plastic parameters with Mohr-Coulomb plasticity was considered for the ballast layer and rock formation. The material parameters for different track layers used in this study are shown in Table-2.

Table 1: Material parameters of different track layers

Layer/Element	Properties
Rails (60 grade rail)	E =200 GPa v=0.2 ρ =7850 kg/m^3
Sleepers	E =30000 MPa v=0.24 ρ =2400 kg/m^3 Dimensions: 2400mm(L)x240mm(W)x240mm(H)
Ballast	E =100 MPa v=0.35 ρ = 1600 kg/m^3 Mohr-Coulomb *$\emptyset_b$=48$^{0\,\#}\varphi$=16^0 Cohesion=10kPa Thickness = 0.3m Shoulder slope = 1:1.5
Rock Mass	*Class-IV Sandstone* *UCS(intact rock)=15MPa* E =500 MPa v=0.25 ρ =1900 kg/m^3 Mohr-Coulomb $\emptyset_b$=40^0, φ=1^0 Cohesion=200kPa Thickness=6m ξ = 0.04
Rock joint	*JCS = 5 MPa* ϵ_{crit} = 5%

4 SIMULATION RESULTS

A total of six combinations of 3 JRC's and 3 planar friction angles ($\emptyset_0$) are considered for analysis in this study. The joint dip is varied from 40 degrees to 90 degrees and the joint displacements of the six combinations are investigated under static railway loads. As explained previously, a single bogie railway load is applied on the railway track, where the equivalent wheel loads from the 4 wheels of the bogie are applied on the top surface of the rails. The joint plane experiences shearing in lateral and longitudinal directions, however due to the orthogonality of the loading direction with strike direction, the joint tries to displace the rock blocks only in the longitudinal direction of the track.

Figure 3 shows the peak joint displacements of the joint under a 30 tonne static railway loading for different dip angles of the joint for the planar friction angle of 20, 30 and 40 degrees with a JRC=2. It can be observed that for a particular joint orientation, the joint displacements increased with lower joint friction angle due to lower shear strength. When the joint is near-vertical, it can be observed that the joint displacements are minimum, and they tend to increase as the dip angle reduces. As the joint becomes steeper, more portion of railway loads is taken by the rock masses instead of the joint, leading to lower mobilized shear stresses on the joint. Further, it is observed that the maximum joint displacement occurs when the joint dip angle is in between 40 and 50 degrees for $\emptyset$ =20^0. For higher $\emptyset$, the dip angle corresponding to maximum joint displacements increased. For cases $\emptyset$=30^0 and 40^0, when the joint dip angle is lower than 50 degrees, the joint displacements tend to reduce again and the joint displacement trend with dip angle shows a concave shape. For a certain magnitude of principal stresses, the shear displacements are inversely proportional to the peak strength and the observed curve of shear displacements is similar to the U-shaped curve from the anisotropic strength theory as described in Fig. 1.

Further, the joint displacements for variation in JRC from 2 to 10 is also plotted in Fig. 3. Increase in JRC contributes to an increase in mobilized friction angle as shown in Eq. 2. Hence, the joint displacement curve shifted down as JRC increased, while also the critical dip angle corresponding to peak displacements shifted to steeper angles. However, it is to be noted that the change in displacements when JRC is increased from 2 to 6 is greater than that when the JRC is further increased from 6 to 10, while no significant change in critical dip angle is observed for the cases of JRC = 6 and 10.

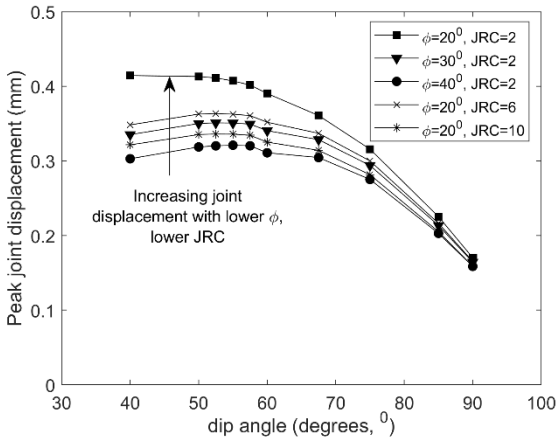

Figure 3. Peak joint displacement on the joint surface for different orientations of joint

However, a slight deviation in the angle corresponding to peak joint displacements is observed when the numerical model results are compared with the traditional anisotropic theory ($\beta_{crit} = 45^0 + \emptyset/2$). This slight discrepancy can be due to the assumptions a simpler triaxial compression stress state considered in the analytical theory, which is more similar to a triaxial compression stress state in the numerical model. Further, due to higher length of the joint, the assumption that the joint is through-going in the analytical theory is not valid for the current problem and significant resistance from the underlying rock layer can increase the strength of the rock formation. This can result in lower critical dip angle when compared to the analytical theory, i.e., at a steeper dip angles the strength of the rock formation is higher at steeper dip angles than expected.

Figure 4 shows the contours of joint displacements for the dip angle of 50 degrees compared with that of 85 degrees. In Fig. 4, the darker parts of the contour show the locations where more joint displacements are mobilized, whereas the lighter regions show lower joint displacements. It can be clearly seen that for joint dip angles in the sliding failure zone, the mobilized shear displacements on the joint gets larger indicating the increased share of train load that is mobilized on to the joint. Further, for dip=50 degrees, shear displacements are propagated to a greater depth where they are restricted to the shallow regions at steeper joint dip angles.

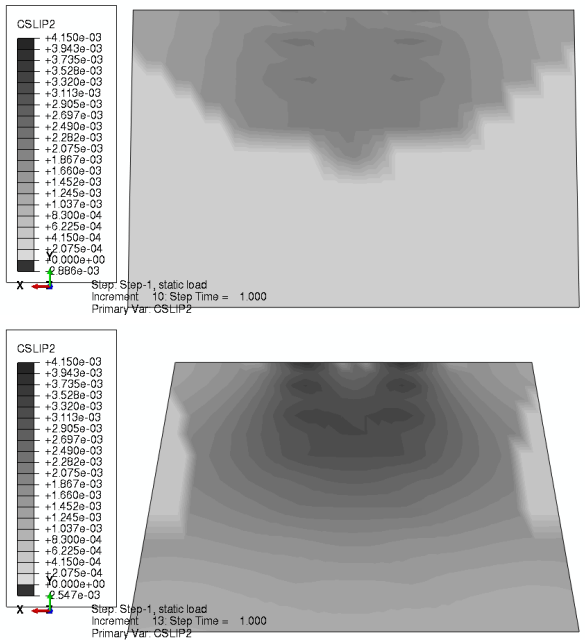

Figure 4. Contours of joint displacements on the joint surface under static railway load: comparison between dip=85^0 and dip=50^0

5 PARAMETRIC STUDY

5.1. Influence of rock mass properties on joint slip

In addition to the joint characteristics, the behavior of joint under railway loading is also dependent on the strength of rock mass in the formation. To investigate the influence of different strengths of rock masses, the mass modulus considered in this study is varied from 200 MPa to 1000 MPa. In Pells (2004), it is mentioned that the rock mass modulus of class-IV sandstone can vary between 50 to 700 MPa while the that of Class-III sandstone will have mass modulus of 350 MPa to 1200 MPa. In this study, the joint displacement behavior is analysed for 4 rock mass modulus ranging from 200 MPa to 1000 MPa. Two JRC's with $\emptyset$=40^0 and the joint with a dip angle of 50 degrees is considered for analysis.

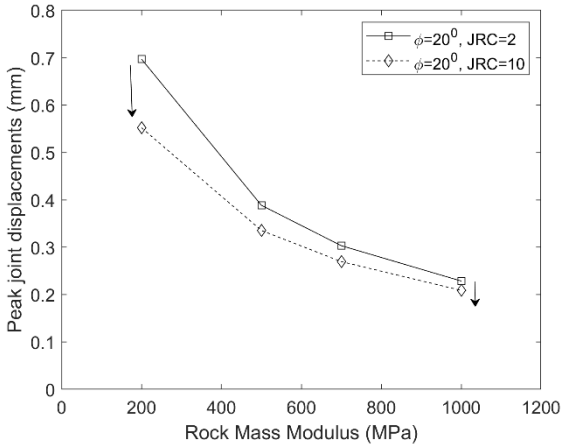

Figure 5. Influence of rock mass modulus on the displacement of joints for joint dip angle = 50^0

Fig. 5 shows the variation of peak joint displacements on the joint surface for different rock mass modulus. Even though the joint characteristics such as $\emptyset$ and JRC are kept constant, higher strength of sliding and resisting rock masses resulted in lower peak joint displacements. The gradient of the curve is found to be higher at lower rock mass moduli signifying the higher influence of a joint in a weak rock. Interestingly, it was observed from Fig. 5 that the influence of JRC was higher when the rock mass is of lower strength, which diminishes gradually as the rock mass strength increases.

5.2. Influence of loading amplitude

Fig. 6 shows the influence of loading amplitude on the displacements of the joints. Typical axle loads of trains in Australia ranging from 15 tonnes to 40 tonnes is considered for analysis. Increase in axle loads only contributed to increase in shear stresses on the joints, which led to increase in joint displacements. For inclinations closer to critical dip angle, the amplification in joint displacements with loading was found to be slightly higher when compared to those with steeper dip angles.

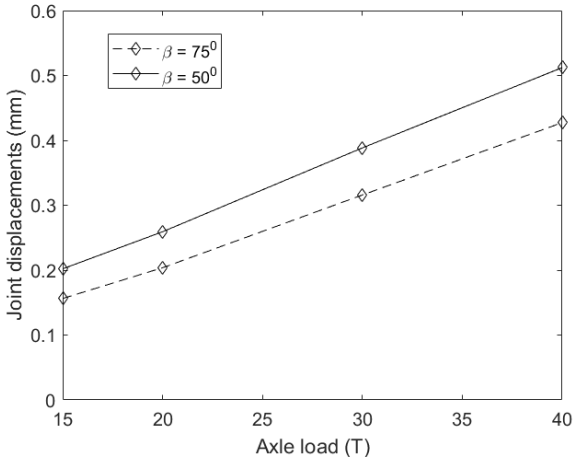

Figure 6. Influence of loading amplitude on the displacement of joints

6 CONCLUSIONS

In this study, the influence of railway loading on the behavior of jointed sandstone rock formation is analysed using a full-scale three-dimensional FEM model. Joint was modelled using a discontinuous interface where the frictional properties are varied considering mobilized frictional coefficient with the JRC of the joint. The track was subjected to static bogie loading with two axles.

Numerical simulations showed that joint dip angle affects the magnitude of joint displacements that occur on a joint. At steeper dip angles ($\beta > 75^0$), much of the railway loading was absorbed by the rock masses while the joint displacements were not affected by change in joint strength characteristics. However, as β varied between 45 and 60 degrees, the influence of railway loads on joint shearing was found to be maximum, which resulted in higher joint displacements. The critical dip angle at which the influence of railway loading was maximum on joint displacements varied slightly with the change in frictional strength of the joint. The model predictions of critical dip angle were compared with the anisotropic strength theory of jointed rocks with a through-going joints. Due to the influence of boundary effects such as base resistance for joint movement and the higher length of the joint, slight deviations in the critical dip angle were observed from those of theoretical model.

Higher JRC values led to lower joint displacements as expected, but the critical dip angle was also found to be changing with JRC. At critical dip angles, the influence of railway loads was extended to greater depths on the joint surface. Under repeated application of railway loads, the surface frictional characteristics of sandstone joints can degrade quickly, and the degradation can also occur at larger depths. This can further increase the difficulty for detecting and mitigation degraded

joints and can lead to the propagation of micro-cracks under further loading.

A parametric study of the influence of different rock mass moduli showed that joints in weaker rock are more susceptible to joint displacements even though the joint roughness characteristics remain same.

7 ACKNOWLEDGEMENTS

The authors would like to acknowledge the financial assistance provided by the Australian Research Council Industrial Transformation Training Centre for Advanced Technologies in Rail Track Infrastructure (ITTC-Rail: IC170100006).

8 REFERENCES

ALEJANO, L. R., GONZÁLEZ-FERNÁNDEZ, M. A., ESTÉVEZ-VENTOSA, X., SONG, F., DELGADO-MARTÍN, J., MUÑOZ-IBÁÑEZ, A., GONZÁLEZ-MOLANO, N. & ALVARELLOS, J. 2021. Anisotropic deformability and strength of slate from NW-Spain. *International Journal of Rock Mechanics and Mining Sciences,* 148**,** 104923.

BANDIS, S., LUMSDEN, A. C. & BARTON, N. R. 1981. Experimental studies of scale effects on the shear behaviour of rock joints. *International Journal of Rock Mechanics and Mining Sciences & Geomechanics Abstracts,* 18**,** 1-21.

BARTON, N. 1973. Review of a new shear-strength criterion for rock joints. *Engineering Geology,* 7**,** 287-332.

BARTON, N. & BANDIS, S. Effects of block size on the shear behavior of jointed rock. The 23rd US symposium on rock mechanics (USRMS), 1982. OnePetro.

BERTUZZI, R. 2014. Sydney sandstone and shale parameters for tunnel design. *Australian Geomechanics Journal,* 49**,** 1-39.

BOBET, A., FAKHIMI, A., JOHNSON, S., MORRIS, J., TONON, F. & YEUNG, M. R. 2009. Numerical Models in Discontinuous Media: Review of Advances for Rock Mechanics Applications. *Journal of Geotechnical and Geoenvironmental Engineering,* 135**,** 1547-1561.

FAIZI, S. A., KWOK, C. Y. & DUAN, K. 2020. The effects of intermediate principle stress on the mechanical behavior of transversely isotropic rocks: Insights from DEM simulations. *International Journal for Numerical and Analytical Methods in Geomechanics,* 44**,** 1262-1280.

HOEK, E. & BROWN, E. T. 1980. Empirical Strength Criterion for Rock Masses. *Journal of the Geotechnical Engineering Division,* 106**,** 1013-1035.

INDRARATNA, B., HAQUE, A. & AZIZ, N. 1999. Shear behaviour of idealized infilled joints under constant normal stiffness. *Géotechnique,* 49**,** 331-355.

INDRARATNA, B., NIMBALKAR, S. & RUJIKIATKAMJORN, C. 2012. Track Stabilisation with Geosynthetics and Geodrains, and Performance Verification through Field Monitoring and Numerical Modelling. *International Journal of Railway Technology,* 1**,** 195-219.

JAEGER, J. C. 1971. Friction of Rocks and Stability of Rock Slopes. *Géotechnique,* 21**,** 97-134.

JING, L. 2003. A review of techniques, advances and outstanding issues in numerical modelling for rock mechanics and rock engineering. *International Journal of Rock Mechanics and Mining Sciences,* 40**,** 283-353.

KENETI, A., POURAGHA, M. & SAINSBURY, B.-A. 2021. Review of design parameters for discontinuous numerical modelling of excavations in the Hawkesbury Sandstone. *Engineering Geology,* 288**,** 106158.

PELLS, P. J. N. 2004. Substance and mass properties for the design of engineering structures in the Hawkesbury Sandstone. *Australian Geomechanics Journal,* 39**,** 1-21.

SELIG, E. T. & WATERS, J. M. 1994. *Track geotechnology and substructure management*, Thomas Telford.

TIEN, Y. M. & KUO, M. C. 2001. A failure criterion for transversely isotropic rocks. *International Journal of Rock Mechanics and Mining Sciences,* 38**,** 399-412.

TIWARI, R. P. & RAO, K. 2007. Response of an anisotropic rock mass under polyaxial stress state. *Journal of materials in civil engineering,* 19**,** 393-403.